THE JOURNAL OF BIOLOGICAL CHEMISTRY VOL. 285, NO. 22, pp. 16830–16843, May 28, 2010
© 2010 by The American Society for Biochemistry and Molecular Biology, Inc. Printed in the U.S.A.

AP-1 (Fra-1/c-Jun)-mediated Induction of Expression of Matrix Metalloproteinase-2 Is Required for 15(*S*)-Hydroxyeicosatetraenoic Acid-induced Angiogenesis*

Received for publication, January 21, 2010, and in revised form, March 23, 2010 Published, JBC Papers in Press, March 29, 2010, DOI 10.1074/jbc.M110.106187

Nikhlesh K. Singh[‡], Dong Van Quyen[‡], Venkatesh Kundumani-Sridharan[‡], Peter C. Brooks[§], and Gadiparthi N. Rao[‡1]

From the [‡]Department of Physiology, the University of Tennessee Health Science Center, Memphis, Tennessee 38163 and the [§]Center for Molecular Medicine, Maine Medical Center Research Institute, Scarborough, Maine 04074

To understand the involvement of matrix metalloproteinases (MMPs) in 15(*S*)-hydroxyeicosatetraenoic acid (15(*S*)-HETE)-induced angiogenesis, we have studied the role of MMP-2. 15(*S*)-HETE induced MMP-2 expression and activity in a time-dependent manner in human dermal microvascular endothelial cells (HDMVECs). Inhibition of MMP-2 activity or depletion of its levels attenuated 15(*S*)-HETE-induced HDMVEC migration, tube formation, and Matrigel plug angiogenesis. 15(*S*)-HETE also induced Fra-1 and c-Jun expression in a Rac1-MEK1-JNK1-dependent manner. In addition, 15(*S*)-HETE-induced MMP-2 expression and activity were mediated by Rac1-MEK1-JNK1-dependent activation of AP-1 (Fra-1/c-Jun). Cloning and site-directed mutagenesis of MMP-2 promoter revealed that AP-1 site proximal to the transcriptional start site is required for 15(*S*)-HETE-induced MMP-2 expression, and Fra-1 and c-Jun are the essential components of AP-1 that bind to MMP-2 promoter in response to 15(*S*)-HETE. Hind limb ischemia led to an increase in MEK1 and JNK1 activation and Fra-1, c-Jun, and MMP-2 expression resulting in enhanced neovascularization and recovery of blood perfusion in wild-type mice as compared with 12/15-Lox$^{-/-}$ mice. Together, these results provide the first direct evidence for a role of 12/15-Lox-12/15(*S*)-HETE axis in the regulation of ischemia-induced angiogenesis.

Angiogenesis has been implicated in the pathogenesis of cancer, diabetic retinopathy, and atherosclerosis (1). On the other hand, a therapeutic role for angiogenesis in the treatment of coronary artery disease and wound healing has been identified (2). In the initiation of new capillaries, endothelial cells of existing blood vessels degrade the underlying basement membrane and invade into the stroma of the neighboring tissue (3, 4). The endothelial cell invasion and migration require the cooperative activity of the plasminogen activator system and the matrix metalloproteinases (MMPs)[2] (3). MMPs were initially discovered in 1962 as collagenolytic activity degrading extracellular matrix protein during tadpole tail resorption (5). Since then, more than 23 members of the MMP family of matrix-degrading enzymes have been identified, characterized, and sub-classified based on their ability to degrade a specific extracellular matrix protein (6). Besides their role in extracellular matrix protein degradation, MMPs have been reported to play a role in the activation of cell surface receptors (7). MMPs not only have been shown to play a role in a number of physiological processes such as embryogenesis (8) and angiogenesis (9, 10), but also have been reported to contribute to the pathogenesis of various diseases, including tumor metastasis (11) and inflammation (12). Among many MMPs, MMP-2 and -9 (also known as gelatinase A and gelatinase B, respectively) have been identified as important players in several cardiovascular diseases, including atherosclerosis, ischemic heart disease, heart failure, aneurysm, and stroke (13–17). MMP-2 is expressed ubiquitously in various cell types, including cardiomyocytes, endothelial cells, fibroblasts, and vascular smooth muscle cells, and plays a crucial role in the regulation of angiogenesis (18–20). Despite the importance of MMPs in cardiovascular development and diseases (21–23), relatively very little is known in regard to the role of these enzymes in eicosanoid-mediated vascular wall remodeling.

It is well established that lipoxygenases, particularly 12/15-lipoxygenase (12/15-Lox), play an important role in the pathogenesis of various vascular diseases and cancers (24–28). One of the initial mechanisms by which 12/15-Lox is implicated in atherosclerosis is its capacity to oxidize low density lipoprotein particles (24). However, many studies also provided clues for additional mechanisms of 12/15-Lox involvement in the pathogenesis of atherosclerosis, restenosis, and cancer. Of these, its role in the regulation of cell growth, migration, and apoptosis have received much attention (29–32). Besides, one of the compelling evidences for the role of 12/15-Lox in atherosclerosis comes from the findings that atherosclerotic arteries produce 15-HETE as a major eicosanoid (33), and its levels are increased in rabbit atherosclerotic arteries (34). Furthermore, the work from our laboratory provided clues for the role of 15(*S*)-HETE in both vascular diseases and cancers. Of note are the observa-

* This work was supported, in whole or in part, by National Institutes of Health Grant HL074860 from NHLBI.

[1] To whom correspondence should be addressed: Dept. of Physiology, the University of Tennessee Health Science Center, 894 Union Ave., Memphis, TN 38163. Tel.: 901-448-7321; Fax: 901-448-7126; E-mail: rgadipar@uthsc.edu.

[2] The abbreviations used are: MMP, matrix metalloproteinase; EMSA, electrophoretic mobility shift assay; 12/15-Lox, 12/15-lipoxygenase; 15(*S*)-HETE, 15(*S*)-hydroxyeicosatetraenoic acid; MAPK, mitogen-activated protein kinase; MEK1, MAPK/extracellular signal-regulated kinase kinase; MEKK, MEK kinase; JNK1, c-Jun N-terminal kinase 1; WT, wild type; siRNA, small interference RNA; GFP, green fluorescent protein; HDMVEC, human dermal microvascular endothelial cell; m.o.i., multiplicity of infection; RT, reverse transcription; nt, nucleotide(s); ChIP, chromatin immunoprecipitation; vWF, van Willebrand factor; dn, dominant negative; FGF, fibroblast growth factor; QRT, quantitative real-time.

tions that 15(*S*)-HETE induces angiogenesis and that this phenomenon requires the autocrine production of angiogenic factors such as vascular endothelial growth factor and interleukin-8 (35, 36). In addition, 15(*S*)-HETE was found to stimulate various signaling molecules, including protein kinase B (Akt), Src, activating transcription factor-2, signal transducer and activator of transcription-3/5, and all of these molecules appear to be involved in the mediation of angiogenesis in response to this stimulus (35–38). During the course of these studies, we also observed that 15(*S*)-HETE activates Rac1, MEK1, and JNK1 in human retinal microvascular endothelial cells facilitating their migration and tube-like structure formation (37, 39). Because MMPs via their capacity to degrade extracellular matrix proteins play a pivotal role in cell migration, one of the major cellular events underlying angiogenesis, we asked the question whether 15(*S*)-HETE stimulates MMPs in microvascular endothelial cells and thereby mediates its angiogenic response. Our results indicate that 15(*S*)-HETE induces the expression of MMP-2 via involving AP-1 (Fra-1/c-Jun) and that MMP-2 activity is required for 15(*S*)-HETE-induced angiogenesis. In support of this conclusion, we also observed that 12/15-Lox$^{-/-}$ mice exhibit decreased MEK1 and JNK1 activation and c-Jun, Fra-1, and MMP-2 expression, thereby reduced angiogenic response following hind limb ischemia as compared with WT mice.

MATERIALS AND METHODS

Reagents—15(*S*)-HETE was bought from Cayman Chemicals (Ann Arbor, MI). Growth factor-reduced Matrigel was obtained from BD Biosciences (Bedford, MA). Phosphospecific anti-JNK1 (Thr-183/Tyr-185) antibodies (cat. no. 9251) and anti-MEK1/2 (Ser-217/221) antibodies (cat. no. 9121) were bought from Cell Signaling Technology (Beverly, MA). Anti-Rac1 antibodies (cat. no. 05–389) and anti-MMP-2 antibodies (cat. no. MAB 3308) were obtained from Upstate Biotechnology (Lake Placid, NY). Anti-β-tubulin antibodies (SC-9104), anti-c-Fos antibodies (SC-52), anti-c-Jun antibodies (SC-44), anti-Fra-1 antibodies (SC-183), anti-Jun-B antibodies (SC-73), anti-JNK1 antibodies (SC-474), anti-MEK1 antibodies (SC-219), and normal rabbit serum (SC-2338) were purchased from Santa Cruz Biotechnology (Santa Cruz, CA). Anti-CD31 antibodies were purchased from BD Pharmingen (Palo Alto, CA). Normal goat serum (cat. no. S-1000) was obtained from Vector Laboratories Inc., (Burlingame, CA). T4 polynucleotide kinase was procured from New England Biolabs (Ipswich, MA). [γ-^{32}P]ATP (3000 Ci/mmol) was bought from Amersham Biosciences (Piscataway, NJ). All the primers were made by IDT (Coralville, IA). Human MMP-2 siRNA (cat. no. ON-TARGETplus SMARTpool L-005959-00, NM_004530), human c-Jun siRNA (cat. no. ON-TARGETplus SMARTpool L-003268-00, NM_002228), human Fra-1 siRNA (cat. no. ON-TARGETplus SMARTpool L-0004341-00, NM_005438), and siCONTROL non-targeting siRNA number 2 (cat. no. D-0012-02-20) and DharmaFECT 2 transfection reagent (cat. no. T-2002-03) were bought from Dharmacon RNAi Technologies (Chicago, IL). All the experiments involving the use of animals were approved by the Animal Care and Use Committee of the University of Tennessee Health Science Center, Memphis, TN.

Adenoviral Vectors—The construction of Ad-GFP, Ad-dnJNK1, Ad-dnMEK1, and Ad-dnRac1 were described previously (38, 39).

Cell Culture—HDMVECs were bought from Cascade Biologics (Portland, OR) and were grown in medium 131 containing microvascular growth supplements, 10 μg/ml gentamycin, and 0.25 μg/ml amphotericin B. Cultures were maintained at 37 °C in a humidified 95% air and 5% CO_2 atmosphere. Cells were quiesced by incubating in medium 131 without microvascular growth supplements for 24 h and used to perform the experiments unless otherwise indicated.

Transfections and Transductions—HDMVECs were transfected with specific siRNA molecules at a final concentration of 100 nM using DharmaFECT 2 transfection reagent according to the manufacturer's instructions. In the case of adenoviral vectors, cells were transduced with adenovirus harboring GFP or target molecule at 40 m.o.i. overnight in complete medium. After transfections or transductions, cells were quiesced for 24 h and used as required.

Gelatin Zymography—Activity of MMP-2 was determined using a gelatin zymography assay. Conditioned medium or tissue extracts containing an equal amount of protein in an equal volume were mixed with an equal volume of non-reducing sample buffer (2% SDS, 125 mM Tris-HCl, pH 6.8, 10% glycerol, and 0.001% bromphenol blue) and electrophoresed onto 10% polyacrylamide gels containing 0.1% gelatin. After electrophoresis, the gels were incubated for 1 h at 37 °C in 2.5% Triton X-100 solution, washed in 50 mM Tris-HCl buffer (pH 7.5) for 30 min, and incubated at 37 °C for overnight in 50 mM Tris-HCl buffer (pH 7.5) containing 200 mM NaCl, 10 mM $CaCl_2$, and 0.05% Brij-35. The gels were stained with 0.05% Coomassie Brilliant Blue G-250 (Bio-Rad) solution containing 2% acetic acid and 45% methanol and then destained with 40% methanol and 10% acetic acid. Gelatinolytic activity was detected as unstained band, and the band intensities were quantified using National Institutes of Health ImageJ.

Quantitative Real-time Reverse Transcriptase-PCR—After appropriate treatments, total cellular RNA was isolated from HDMVECs or tissues by using a RiboPure™ kit (Ambion, Austin, TX) or an RNeasy Fibrous Tissue Mini Kit (Qiagen, Valencia, CA), respectively, as per the manufacturers' guidelines. Reverse transcription was carried out with a High Capacity cDNA reverse transcription kit for reverse transcription (RT)-PCR based on the supplier's protocol (Applied Biosystems, Foster City, CA). The cDNA was then used as a template for PCR amplification using TaqMan Gene Expression Assays for human MMP-2 (Hs01548724_m1), mouse MMP-2 (Mm00439506_m1), human β-actin (Hs99999903_m1), and mouse β-actin (Mm02619580_g1). The amplification was carried out on 7300 Real-Time PCR Systems (Applied Biosystems) using the following conditions: 95 °C for 10 min followed by 40 cycles at 95 °C for 15 s with extension at 60 °C for 1 min for both MMP-2 and β-actin. The PCR amplification run was examined, using the 7300 real-time PCR system-operated SDS version 1.4 program. The program uses the Delta Rn analysis method (Applied Biosystems).

Cell Migration Assay—Cell migration was performed using a modified Boyden chamber method (38). The cell culture inserts containing membranes with 10 mm diameter and 8.0-μm pore size (Nalgene Nunc International, Rochester, NY) were placed in a 24-well tissue culture plate (Costar, Corning Inc., Corning, NY). The lower surface of the porous membrane was coated with 70% Matrigel at 4 °C overnight and then blocked with 0.1% heat-inactivated bovine serum albumin at 37 °C for 1 h. HDMVECs were quiesced for 24 h in medium 131, trypsinized, and neutralized with trypsin-neutralizing solution. Cells were seeded into the upper chamber at 1×10^5 cells/well. Vehicle or 15(*S*)-HETE was added to the lower chamber. Both the upper and lower chambers contained medium 131. When the effect of a pharmacological inhibitor was tested on 15(*S*)-HETE-induced HDMVEC migration, cells were incubated with the inhibitor for 30 min first and then added to the upper chamber. In the siRNA approach, cells were transfected with scrambled or specific siRNA and quiesced before they were subjected to migration assay. After 8 h of incubation at 37 °C, non-migrated cells were removed from the upper side of the membrane with cotton swabs, and the cells on the lower surface of the membrane were fixed in methanol for 15 min. The membrane was then stained with 4′,6-diamidino-2-phenylindole in Vectashield mounting medium (Vector Laboratories Inc.) and observed under a diaphot fluorescence microscope with a photometrics CH250 charge-coupled device camera (Nikon, Garden City, NY). Cells were counted in five randomly selected fields per well and presented as the number of migrated cells/field.

Tube Formation Assay—Tube formation assay was performed as described previously (38). Twenty-four well culture plates (Costar, Corning Inc.) were coated with growth factor-reduced Matrigel (BD Biosciences) in a total volume of 280 μl/well and allowed to solidify for 30 min at 37 °C. HDMVECs were trypsinized, neutralized with trypsin-neutralizing solution, and resuspended in medium 131 at 5×10^5 cells/ml, and 200 μl of this cell suspension was added into each well. Vehicle or 15(*S*)-HETE, at the indicated concentration, was added to the appropriate well, and the cells were incubated at 37 °C for 6 h. When the effect of a pharmacological inhibitor was tested on 15(*S*)-HETE-induced HDMVEC tube formation, cells were incubated with the inhibitor for 30 min first and then plated. In the siRNA approach, cells were transfected with scrambled or specific siRNA and quiesced before they were subjected to tube formation assay. Tube formation was observed under an inverted microscope (Eclipse TS100, Nikon). Images were captured with a charge-coupled device color camera (KP-D20AU, Hitachi, Japan) attached to the microscope, and tube length was measured using ImageJ.

Western Blot Analysis—After appropriate treatments and rinsing with cold phosphate-buffered saline, HDMVECs were lysed in 500 μl of lysis buffer (phosphate-buffered saline, 1% Nonidet P-40, 0.5% sodium deoxycholate, 0.1% SDS, 100 μg/ml phenylmethylsulfonyl fluoride, 100 μg/ml aprotinin, 1 μg/ml leupeptin, and 1 mM sodium orthovanadate) and scraped into 1.5-ml Eppendorf tubes. Tissues extracts were prepared by homogenization using Tissue Tearor (Biospec Products Inc.) in the above mentioned lysis buffer. After standing on ice for 20 min, the cell and tissue extracts were cleared by centrifugation at 12,000 rpm for 20 min at 4 °C. The cell and tissue extracts containing equal amounts of protein were resolved by electrophoresis on 0.1% SDS and 10% polyacrylamide gels. The proteins were transferred electrophoretically to a nitrocellulose membrane (Hybond, Amersham Biosciences). After blocking in 10 mM Tris-HCl buffer, pH 8.0, containing 150 mM NaCl, 0.1% Tween 20, and 5% (w/v) nonfat dry milk, the membrane was treated with appropriate primary antibodies followed by incubation with horseradish peroxidase-conjugated secondary antibodies. The antigen-antibody complexes were detected using chemiluminescence reagent kit (Amersham Biosciences).

Pull-down Assay—An equal amount of protein from control and each treatment was incubated with glutathione *S*-transferase-p21-activated kinase (Cdc42 and Rac1 interactive binding domain)-conjugated Sepharose CL4B beads for 45 min at 4 °C. The beads were collected by centrifugation, washed in lysis buffer and heated in Laemmli sample buffer for 5 min, and the released proteins were resolved on 0.1% SDS-12% PAGE and analyzed by immunoblotting for Rac1 levels using anti-Rac1 antibodies.

Cloning of Human MMP-2 Promoter—The human MMP-2 promoter region −1704 to +14 nt relative to transcription start site (40) was PCR-amplified from genomic DNA using primers, forward: 5′-TACGGGGTACCCCCTCCCAAGAGGGTCC-3′ and reverse: 5′-ACGTCGAAGCTTGGATGCAGCGGAAACAAGG-3′, with the underlines indicating the restriction enzyme sites KpnI and HindIII, respectively. The PCR products were digested with KpnI and HindIII, purified by gel extraction kit (Qiagen) and cloned into the pGL3 basic vector (Promega, Madison, WI) at the same sites yielding MMP2p-WT-Luc. Site-directed mutations in the first (−1263 to −1270 nt), second (−1615 to −1621 nt), and the third (−1673 to −1679 nt) AP-1 binding sites were introduced by QuikChange site-directed mutagenesis kit (Stratagene, La Jolla, CA) following the manufacturer's instructions using the following primers, forward: 5′-GGTCTCAGCTCAGAAGcagCTTCTTCCAGGAAGC-3′ and reverse: 5′-GCTTCCTGGAAGAAGctgCTTCTGAGCTGAGACC-3′; forward: 5′-ACTTGTCTGAAGCCCcagGAGACCCAAGCCGCAG-3′ and reverse: 5′-CTGCGGCTTGGGTCTCctgGGGCTTCAGACAAGT-3′; forward: 5′-GAGGGTCCTTTAAAACgtcCTCTGGAAAGTCAGAG-3′ and reverse: 5′-CTCTGACTTTCCAGAGgacGTTTTAAAGGACCCTC-3′, respectively. The lowercase letters indicate the mutations. The nucleotide sequence of each construct was verified by DNA sequencing.

Luciferase Assay—HDMVECs were transfected with MMP-2 promoter-luciferase constructs or pGL3 basic vector using Lipofectamine 2000 reagent. After growth synchronization in growth factor free-medium for 24 h, cells were treated with and without 15(*S*)-HETE (0.1 μM) for 8 h. Cells were then washed once with ice-cold phosphate-buffered saline and lysed with 200 μl of lysis buffer. The cell extracts were collected into microcentrifuge tubes and centrifuged for 2 min at 12,000 $\times$ *g* at 4 °C. The supernatants were collected and assayed for luciferase activity using Luciferase Assay System (Promega) and a single tube luminometer (TD20/20 Turner Designs, Sunnyvale, CA), and the values are expressed as relative luciferase units.

Electrophoretic Mobility Shift Assay—After appropriate treatments, nuclear extracts were prepared from HDMVECs as

described previously (36). The protein content of the nuclear extracts was determined using a Micro BCA Protein Assay Reagent Kit (Pierce). Protein-DNA complexes were formed by incubating 5 μg of nuclear protein in a total volume of 20 μl consisting of 15 mM HEPES, pH 7.9, 3 mM Tris-HCl, pH 7.9, 60 mM KCl, 1 mM EDTA, 1 mM phenylmethylsulfonyl fluoride, 1 mM dithiothreitol, 2.5 μg/ml bovine serum albumin, 1 μg/ml poly(dI-dC), 15% glycerol, and 100,000 cpm of ^{32}P-labeled oligonucleotide probe for 30 min on ice. The protein-DNA complexes were resolved by electrophoresis on 4% polyacrylamide gel using 1× Tris-glycine-EDTA buffer (25 mM Tris-HCl, pH 8.5, 200 mM glycine, 0.1 mM EDTA). Double-stranded oligonucleotides from −1252 nt to −1282 nt region of human MMP-2 promoter (accession no. AJ298926) (5′-CCTGGAAGAAGTGACTTCTGAGCTGAGACCT-3′ and 3′-GGACCTTCTTCACTGAAGACTCGACTCTGGA-5′) were used as ^{32}P-labeled oligonucleotide probes to measure AP-1 DNA-binding activities. Double-stranded oligonucleotides were labeled with [γ-^{32}P]ATP using the T4 polynucleotide kinase kit following the supplier's protocol.

Chromatin Immunoprecipitation Assay—Chromatin immunoprecipitation (ChIP) assay was performed on HDMVECs using ChIP assay kit following the supplier's protocol (Upstate Biotechnology). AP-1 DNA complexes were immunoprecipitated using anti-Fra-1 antibodies or anti-c-Jun antibodies. Preimmune rabbit serum was used as a negative control. The immunoprecipitated DNA was uncross-linked, subjected to proteinase K digestion, and purified using QIAquick columns (Qiagen). The purified DNA was used as a template for PCR amplification using primers (forward, 5′-CTTCTCAAACTGTTCCCTGC-3′; reverse, 5′-GGAACGCCTGACTTCAGC-3′) flanking the putative AP-1 located at −1263 and −1270 in human MMP-2 promoter region (accession no. AJ298926). The PCR products were resolved on 1.5% agarose gels and visualized by ethidium bromide staining.

Matrigel Plug Angiogenesis Assay—A Matrigel plug assay was performed essentially as described previously (36). The C57BL/6 and 12/15-LOX$^{-/-}$ mice were obtained from the Jackson Laboratory (Bar Harbor, ME). C57BL/6 (WT) mice or 12/15-LOX$^{-/-}$ mice (8 weeks old) were lightly anesthetized with ketamine (100 mg/kg) and xylazine (8 mg/kg) and were injected subcutaneously with 0.5 ml of Matrigel, which was premixed with vehicle or 5 μM of 15(*S*)-HETE along the abdominal midline. The injections were made rapidly with a 30-gauge 1/2 needle to ensure the entire content was delivered as a single plug. Wherever the effect of a pharmacological inhibitor was tested on 15(*S*)-HETE-induced angiogenesis, it was added to the Matrigel prior to injecting into mice. The mice were allowed to recover, and 7 days later, unless otherwise stated, the animals were sacrificed by inhalation of CO_2; the Matrigel plugs were harvested from underneath the skin. The plugs were homogenized in 1 ml of deionized H_2O on ice and cleared by centrifugation at 10,000 rpm for 6 min at 4 °C. The supernatant was collected and used in duplicate to measure hemoglobin content with Drabkin's reagent along with hemoglobin standard essentially according to the manufacturer's protocol (Sigma). The absorbance was read at 540 nm in a Microplate reader (Spectra Max 190, Molecular Devices, Sunnyvale, CA). These experiments were repeated at least three times with six mice for each group, and the values are expressed as grams hemoglobin/dl/mg of plug.

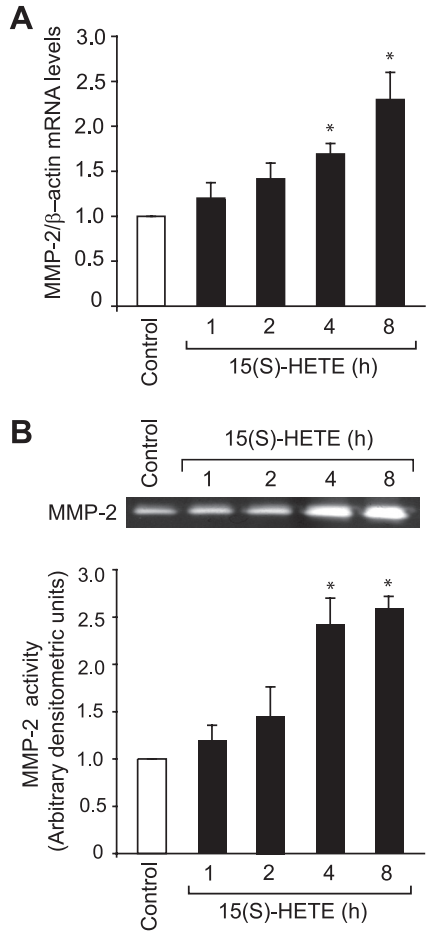

FIGURE 1. **15(*S*)-HETE induces MMP-2 expression and activity.** *A* and *B*, quiescent HDMVECs were treated with and without 0.1 μM 15(*S*)-HETE for the indicated time periods, and either total cellular RNA was isolated and analyzed for MMP-2 and β-actin mRNA levels by QRT-PCR (*A*) or medium was collected and analyzed for MMP-2 activity by gelatin zymography (*B*). The *bar graphs* in *A* and *B* represent the mean ± S.D. values of three independent experiments. *, $p < 0.01$ *versus* control.

Hind Limb Ischemia—Hind limb ischemia was induced in wild-type and 12-LOX$^{-/-}$ mice by ligating the left common femoral artery proximal to the origin of the profunda femoris artery (41). Mice were anesthetized with intraperitoneal injection of ketamine (100 mg/kg) and xylazine (8 mg/kg). An incision was made in the left groin of mice, and blunt dissection was performed to identify the left common femoral artery by its pale pink color and pulsatile nature. The common femoral vein and femoral nerve were separated from the artery. Two ligations were performed in the common femoral artery proximal to the origin of the profunda femoris artery using 6-0 nylon sutures. The common femoral artery was then transected between the ligation sites. Immediate blanching was noted in the distal left hind limb after ligation. The incision was sutured in a single layer using the same suture material as for ligation. Mice were noted to be limping and dragging the left hind limb after recovery from anesthesia. After 7 days, mice were anesthetized and placed on a heating pad (~37 °C), and the limb blood perfusion was measured by Laser Doppler Imager System (Laser

Doppler Perfusion Imager System, moorLDI-2HR, Moor Instruments, Wilmington, DE). Perfusion was expressed as the ratio of ischemic to non-ischemic hind limb perfusion. In parallel experiments, mice were sacrificed, adductor muscles from ischemic and non-ischemic limbs of wild type and 12/15-Lox$^{-/-}$ mice were dissected out, and either protein or RNA was isolated or embedded in OCT compound. Tissue extracts were analyzed for MEK1 and JNK1 phosphorylation and Fra-1, c-Jun, and MMP-2 levels. Total RNA was used to measure MMP-2 expression. Embedded tissues were sectioned and stained for CD31, vWF, and Hu177.

Double Immunofluorescence Staining—After retrieving the Matrigel plugs and adductor muscles from mice, they were snap-frozen in OCT compound. Cryosections (5 μm) were made using Leica Kryostat (Model CM3050S, Leica, Wetzlar, Germany). After blocking in normal goat serum, the cryosections were incubated with rabbit anti-mouse von Willebrand Factor (vWF) antibodies and rat anti-mouse CD31 antibodies or monoclonal Hu177 antibodies (42) and rat anti-mouse CD31 for 1 h (1:500). After washing in phosphate-buffered saline, all slides were incubated with goat anti-rabbit secondary antibodies conjugated with Alexa Fluor 568 or goat anti-rat secondary antibodies conjugated with Alexa Fluor 488 or goat anti-rat secondary antibodies conjugated with Alexa Fluor 568 or goat anti-mouse secondary antibodies conjugated with Alexa Fluor 488. Fluorescence was observed under a Zeiss inverted microscope (Model AxioVision AX10).

Statistics—All the experiments were repeated three times, and data are presented as mean ± S.D. The treatment effects were analyzed by Student t test, and the p values <0.01 were considered statistically significant. In the case of double immunofluorescence staining, ChIP analysis, EMSA, gelatin zymography, and Western blotting, one representative set of data is shown.

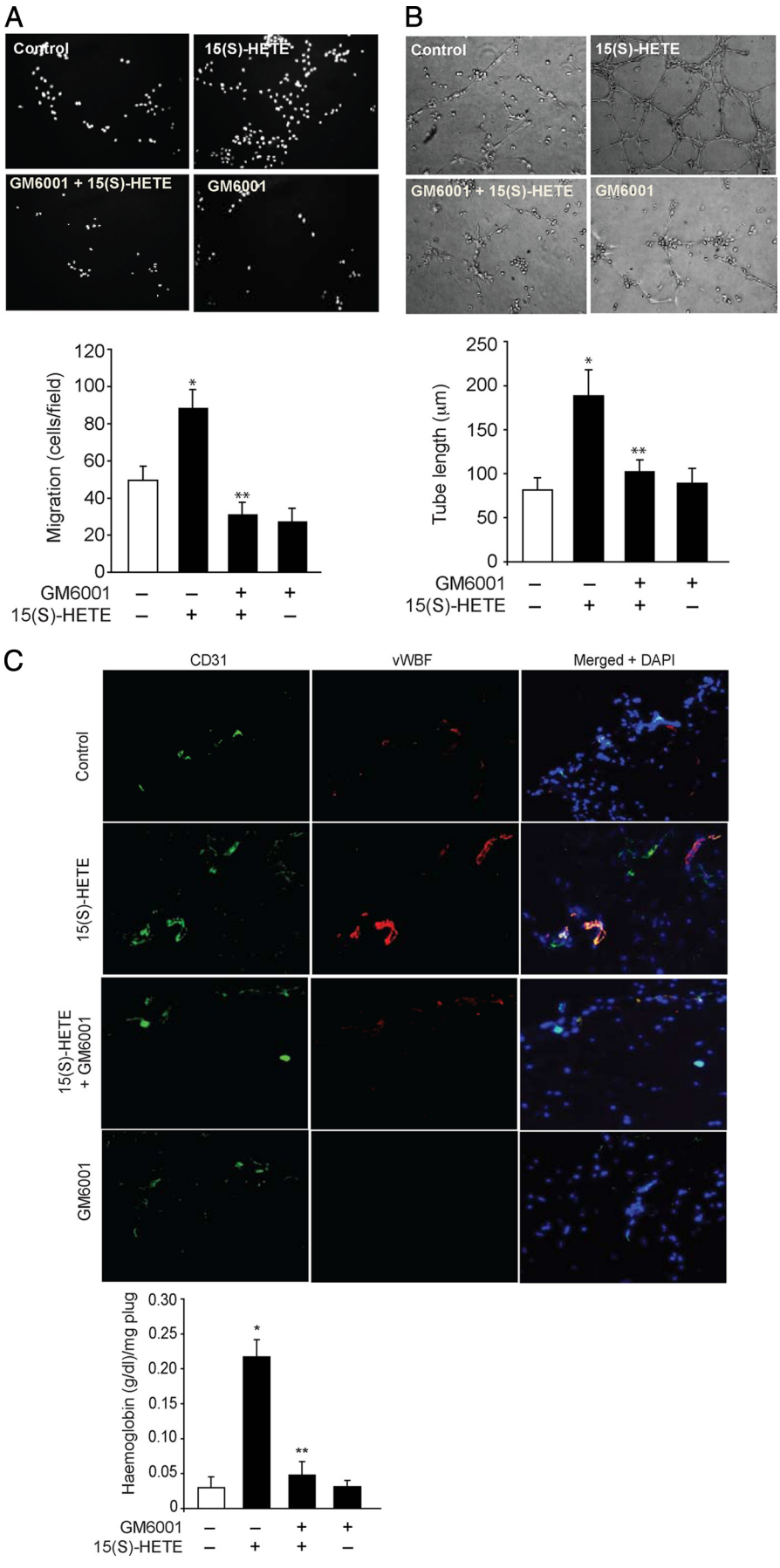

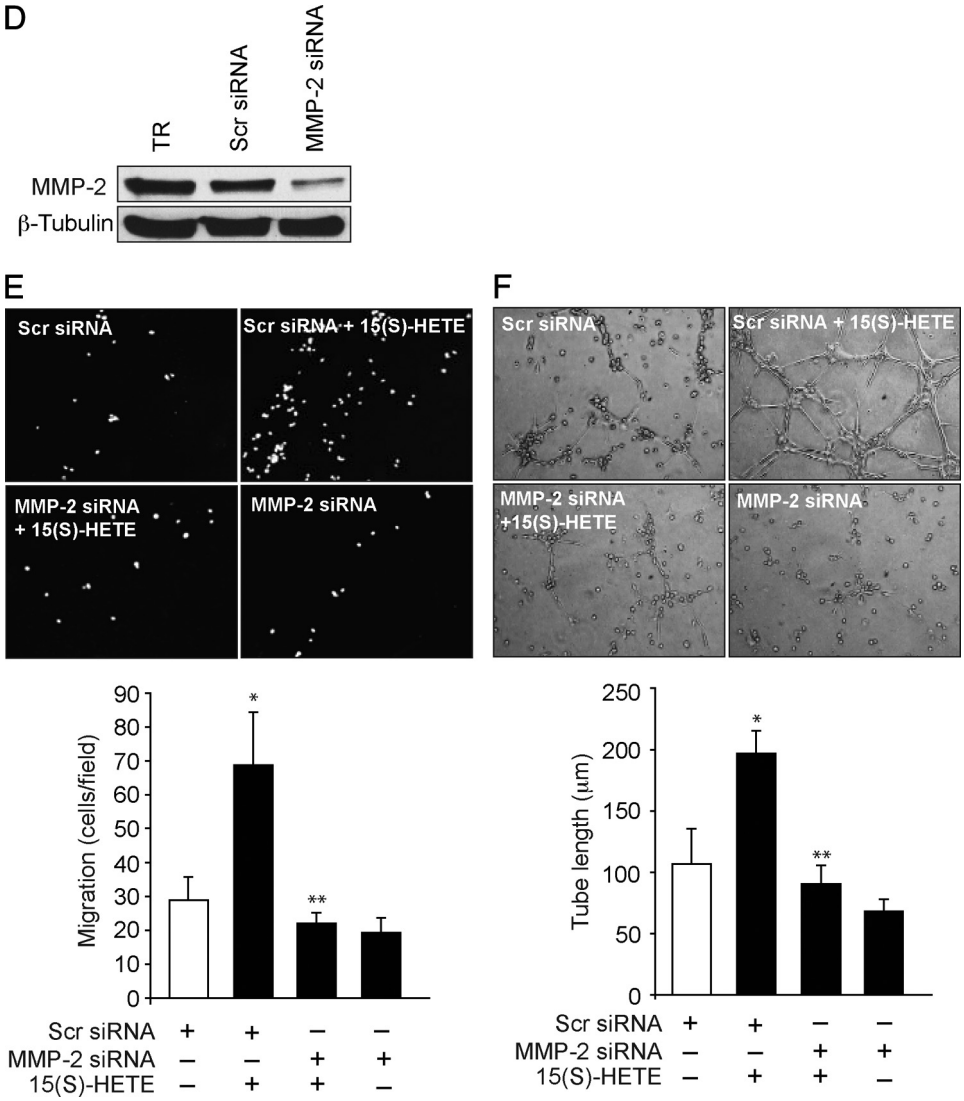

FIGURE 2—*continued*

RESULTS

15(S)-HETE Induces MMP-2 Expression and Activation in HDMVECs—To understand the mechanisms of 15(*S*)-HETE-induced angiogenesis, we studied the role of MMP-2. 15(*S*)-HETE (0.1 μM)-induced MMP-2 mRNA levels in a time-dependent manner with a 2.5-fold increase at 8 h compared with control (Fig. 1*A*). To confirm these results, we also studied the time course effect of 15(*S*)-HETE on MMP-2 activity. As measured by gelatin zymography, we found that treatment with 15(*S*)-HETE (0.1 μM) led to a time-dependent release of MMP-2 into the conditioned medium with 2.5-fold increase at 8 h as compared with untreated cells (Fig. 1*B*).

MMP-2 Mediates 15(S)-HETE-induced HDMVEC Migration, Tube Formation, and Matrigel Plug Angiogenesis—To test the role of MMP-2 in 15(*S*)-HETE-induced angiogenesis, we have studied the effect of GM6001, a potent inhibitor of MMPs (43) on 15(*S*)-HETE-induced HDMVEC migration, tube formation, and Matrigel plug angiogenesis. 15(*S*)-HETE stimulated both HDMVEC migration and tube formation approximately by 2.0- to 2.5-fold as compared with control, and GM6001 completely blocked these effects (Fig. 2, *A* and *B*). GM6001 also attenuated the basal HDMVEC migration to some extent. Similarly, 15(*S*)-HETE (10 μM) induced Matrigel plug angiogenesis by 3-fold as compared with vehicle control, and GM6001 significantly inhibited this effect as well (Fig. 2*C*). Because GM6001 inhibits the activity of several MMPs, including MMP-2 and MMP-9, to validate the role of MMP-2 in 15(*S*)-HETE-induced angiogenesis, we next used an siRNA approach. Depletion of MMP-2 levels by its siRNA attenuated the effect of 15(*S*)-HETE on both HDMVEC migration and tube formation (Fig. 2, *D–F*).

15(S)-HETE-induced MMP-2 Expression and Activity Require Activation of Rac1, MEK1, and JNK1 in HDMVECs—Members of the Rho family of small GTPases play an important role in a variety of cellular processes, including cell migration and proliferation (44–46). Rac1, a member of the Rho family of GTPases, has been shown to mediate activation of MMP-2 during cell invasion through a collagen barrier (47). Previously we have shown that 15(*S*)-HETE activates the Rac1-MEK-1-JNK1 signaling axis in human retinal microvascular endothelial cells (38). To further characterize the role of Rac1, MEK1, and JNK1 in 15(*S*)-HETE-induced angiogenesis, here we have tested their involvement in 15(*S*)-HETE-stimulated MMP-2 expression. Consistent with our previous findings, 15(*S*)-HETE stimulated Rac1,

FIGURE 2. **MMP-2 mediates 15(*S*)-HETE-induced HDMVEC migration and tube formation *in vitro* and Matrigel plug angiogenesis *in vivo*.** *A* and *B*, quiescent HDMVECs were treated with and without 10 mM GM6001 for 30 min at 37 °C, trypsinized, rinsed with trypsin-neutralizing solution, and subjected to 0.1 μM 15(*S*)-HETE-induced migration (*A*) or tube formation (*B*). *C*, WT mice were injected subcutaneously with 0.5 ml of Matrigel premixed with vehicle or 10 μM 15(*S*)-HETE with and without 10 mM GM6001. One week later, the animals were sacrificed, and the Matrigel plugs were harvested from underneath the skin, and either cryosections were made and examined by double immunofluorescence staining for vWF and CD31 using their specific antibodies or analyzed for hemoglobin content using Drabkin's reagent. *D*, HDMVECs were transfected with scrambled or MMP-2 siRNA, and 48 h later cell extracts were prepared and analyzed by Western blotting for MMP-2 levels using its specific antibodies. *E* and *F*, all the conditions were the same as in *D* except that, after transfection, HDMVECs were quiesced and subjected to 15(*S*)-HETE (0.1 μM)-induced migration (*E*) or tube formation (*F*). The *bar graphs* in *A–F* represent the mean ± S.D. values of three independent experiments or six plugs from six animals. *, $p < 0.01$ *versus* control; **, $p < 0.01$ *versus* 15(*S*)-HETE. *TR*, transfection reagent.

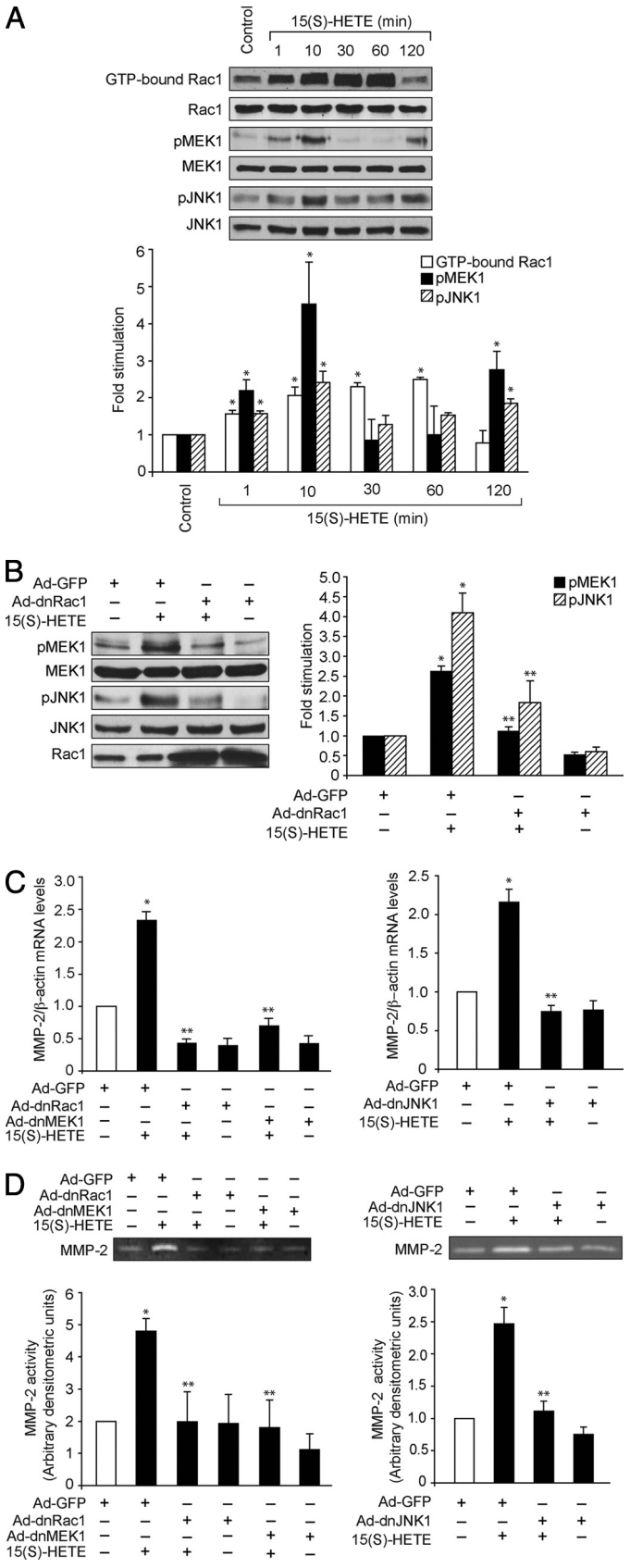

FIGURE 3. **Rac1, MEK1, and JNK1 mediate 15(*S*)-HETE-induced MMP-2 expression and activity.** *A*, quiescent HDMVECs were treated with and without 0.1 μM 15(*S*)-HETE for the indicated time periods, and cell extracts were prepared and analyzed for Rac1 activation by pulldown assay and MEK1 and JNK1 phosphorylation by Western blotting using their phosphospecific antibodies. Whereas total cellular levels of Rac1 are shown in the *second blot* from the *top*, the pMEK1 and pJNK1 blots were reprobed with anti-MEK1 and anti-JNK1 antibodies for normalization. *B*, HDMVECs were transduced with Ad-GFP or Ad-dnRac1 at 40 m.o.i., quiesced, treated with and without 15(*S*)-HETE (0.1 μM) for 10 min, and MEK1 and JNK1 phosphorylation were measured. The blots were reprobed with anti-MEK1 or anti-JNK1 antibodies for normalization. One of these blots was reprobed with anti-Rac1 antibodies to show the overexpression of dnRac1. *C* and *D*, HDMVECs were transduced with Ad-GFP, Ad-dnRac1, Ad-dnMEK1, or Ad-dnJNK1 at 40 m.o.i., quiesced, treated with and without 15(*S*)-HETE (0.1 μM) for 8 h and either total cellular RNA was isolated and analyzed for MMP-2 and β-actin mRNA levels by QRT-PCR (*C*) or medium was collected and assayed for MMP-2 activity by gelatin zymography (*D*). The *bar graphs* in *A–D* represent mean ± S.D. values of three independent experiments. *, $p < 0.01$ *versus* control or Ad-GFP; **, $p < 0.01$ *versus* 15(*S*)-HETE or Ad-GFP plus 15(*S*)-HETE.

MEK1, and JNK1 activation in a time-dependent manner with a 2- to 3-fold increase at 10 min (Fig. 3*A*). It was observed that, although Rac1 activation sustained for ~1 h, both MEK1 and JNK1 showed a biphasic activation with a first and heightened peak at 10 min and a second peak after 2 h. In addition, blockade of Rac1 via forced expression of its dominant negative mutant substantially inhibited 15(*S*)-HETE-induced MEK1 and JNK1 phosphorylation (Fig. 3*B*). To test the role of Rac1, MEK1, and JNK1 in 15(*S*)-HETE-induced MMP-2 expression, we have used a dominant negative mutant approach. Adenovirus-mediated expression of dnRac1, dnMEK1, or dnJNK1 blocked 15(*S*)-HETE-induced MMP-2 expression and activity (Fig. 3, *C* and *D*).

15(S)-HETE Activates AP-1 via Rac1-MEK1-JNK1 Signaling in HDMVECs—Based on the identification of the AP-1 binding sites in the collagenase promoter, this transcriptional factor has been implicated as a direct regulator of MMP activity (48, 49). To determine whether AP-1 is involved in 15(*S*)-HETE-induced MMP-2 expression and activity, we have studied first the time course effects of 15(*S*)-HETE on expression of various Fos and Jun family of proto-oncogenes, the AP-1 subunits, in HDMVECs. As shown in Fig. 4*A*, exposure of HDMVECs to 15(*S*)-HETE (0.1 μM) caused a rapid induction of c-Fos, Fra-1, c-Jun, and Jun-B levels with ~2- to 3-fold increase at 1 h. Blockade of Rac1 or MEK1 by adenovirus-mediated expression of their dominant negative mutants while affecting the levels of c-Fos and Jun-B to some extent significantly blunted the levels of Fra-1 and c-Jun induced by 15(*S*)-HETE (Fig. 4*B*). Similarly, adenovirus-mediated expression of dnJNK1 attenuated 15(*S*)-HETE-induced Fra-1 and c-Jun levels. Based on these results, we next tested the role of Fra-1 and c-Jun on 15(*S*)-HETE-induced MMP-2 expression and activity. Depletion of Fra-1 or c-Jun levels by their respective siRNAs blocked 15(*S*)-HETE-induced expression and activity of MMP-2 (Fig. 4, *C–E*).

To test whether AP-1 binds to MMP-2 promoter in response to 15(*S*)-HETE, we cloned a 1.7-kb human MMP-2 promoter region and identified three putative AP-1 binding sites located each at −1263, −1615, and −1673 nt relative to the transcription start site by Transfac analysis (Fig. 5*A*). Promoter-luciferase reporter gene assays along with site-directed mutagenesis showed that the AP-1 site proximal to the transcriptional start site is important for 15(*S*)-HETE-induced MMP-2 expression (Fig. 5*B*). To identify the AP-1 components in 15(*S*)-HETE-induced MMP-2 promoter-luciferase activity, we next tested the role of Fra-1 and c-Jun. Down-regulation of either Fra-1 or c-Jun levels by their respective siRNAs significantly attenuated

15(*S*)-HETE-induced MMP-2 promoter-luciferase activity (Fig. 6*A*). To confirm these observations, we also studied a time course effect of 15(*S*)-HETE on AP-1 DNA-binding activity using an AP-1 element at −1263 nt as a ^{32}P-labeled probe. 15(*S*)-HETE induced AP-1 DNA-binding activity in a time-dependent manner with ~3-fold increase at 1 h (Fig. 6*B*). Blockade of Rac1-MEK1 signaling by adenovirus-mediated expression of their dominant negative mutants completely inhibited 15(*S*)-HETE-induced AP-1 DNA-binding activity (Fig. 6*C*). To obtain additional evidence for the role of Fra-1 and c-Jun in the regulation of MMP-2 promoter activity, we performed a ChIP assay. ChIP analysis revealed a time-dependent binding of Fra-1 and c-Jun to MMP-2 promoter *in vivo* (Fig. 6*D*). In addition blockade of Rac1 or MEK1 via adenovirus-mediated expression of their dominant negative mutants suppressed the binding of Fra-1 and c-Jun to MMP-2 promoter *in vivo* (Fig. 6*E*).

Lack of a Neovascularization Response in 12/15-Lox$^{-/-}$ Mice following Hind Limb Ischemia—To demonstrate the *in vivo* relevance of the *in vitro* findings, we used a murine model of hind limb ischemia. It was observed that, as compared with WT mice, 12/15-Lox$^{-/-}$ mice had impaired recovery of blood flow 7 days after hind limb ischemia (Fig. 7*A*). To confirm these results further, immunofluorescence was performed on the adductor muscles of both WT and 12/15-Lox$^{-/-}$ mice for the presence of endothelial cells. Double immunofluorescence staining demonstrated the presence of increased CD31 and vWF in the ischemic muscles of WT mice as compared with 12/15-Lox$^{-/-}$ mice (Fig. 7*B*). To understand the signaling events of neovascularization *in vivo*, we have also measured the activation of MEK1 and JNK1 in the adductor muscles of WT and 12/15-Lox$^{-/-}$ mice with and without ischemia. As compared with non-ischemia control, ischemia induced both MEK1 and JNK1 phosphorylation at least by 2-fold in WT mice (Fig. 8*A*). Similarly, ischemia induced Fra-1, c-Jun, and MMP-2 expression as well as MMP-2 activity by 2- to 5-fold in the adductor muscles of WT mice (Fig. 8, *B–E*). Surprisingly, as compared with WT mice, ischemia failed to stimulate the acti-

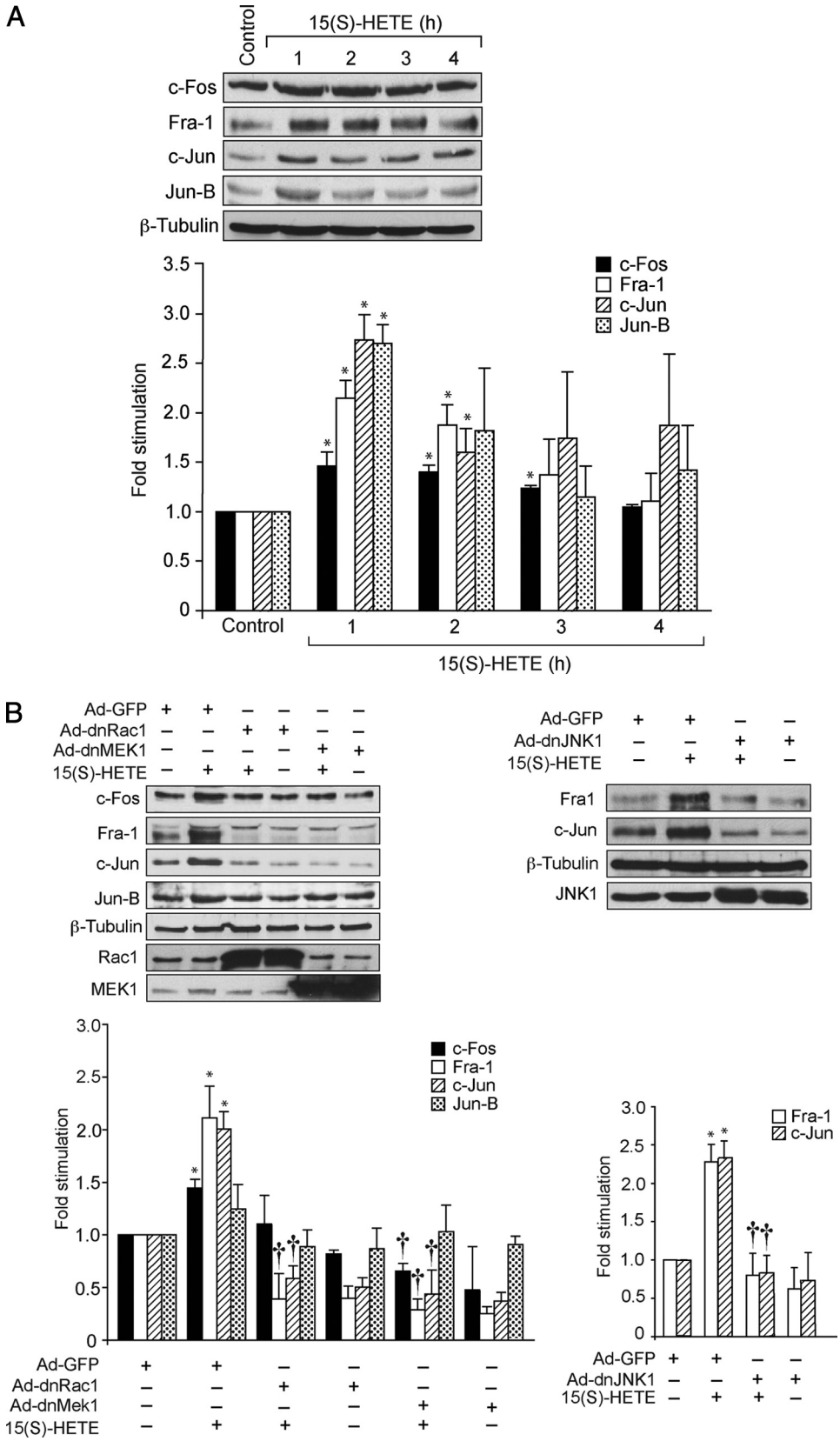

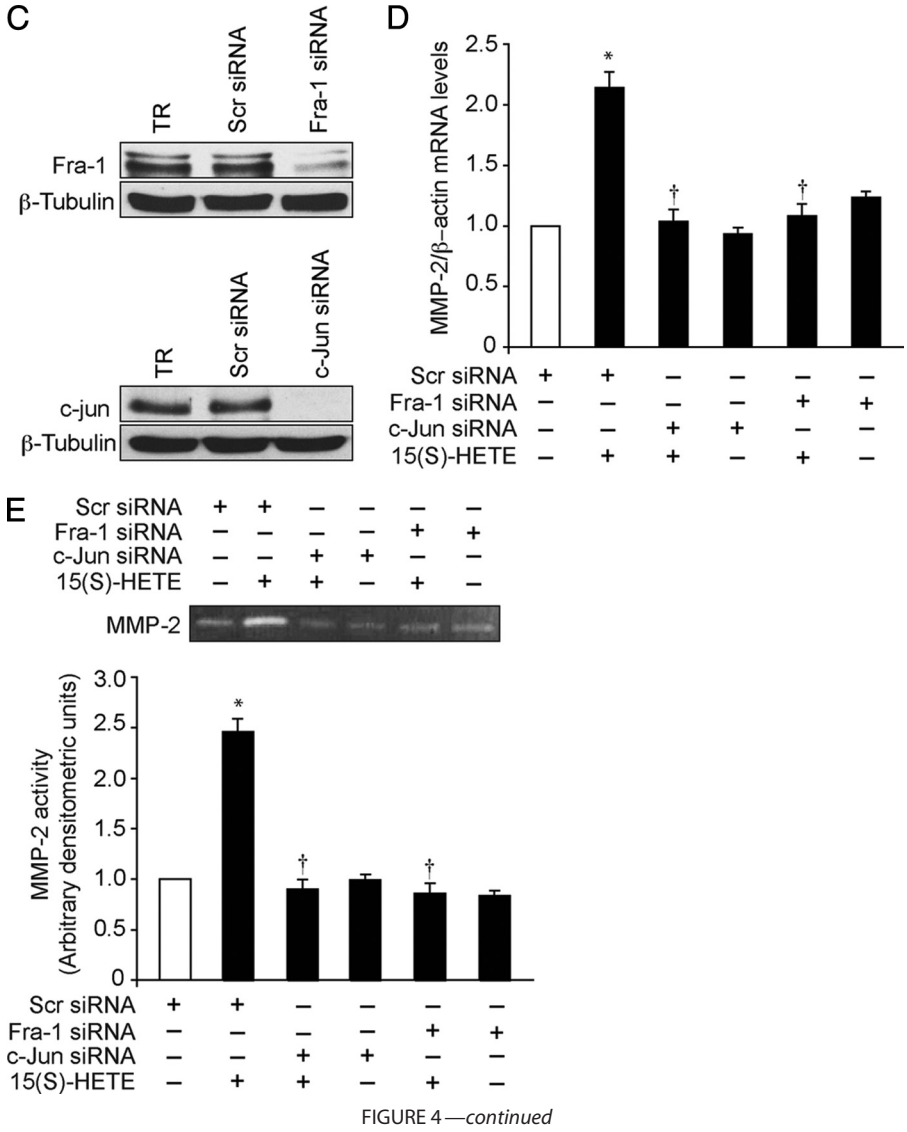

FIGURE 4—*continued*

vation of MEK1 and JNK1 as well the induction of expression of Fra-1, c-Jun, and MMP-2 in the adductor muscles of 12/15-Lox$^{-/-}$ mice. Consistent with a lack of effect on MMP-2 levels, ischemia also had no significant effect on MMP-2 activity in 12/15-Lox$^{-/-}$ mice. HU177 was selectively exposed in the interstitial matrix of tumors as well as in the extracellular matrix of angiogenic blood vessels as a result of extracellular matrix degradation by MMPs (42). To confirm the role of MMP-2 in ischemia-induced neovascularization, we also performed double immunofluorescence staining for Hu177 and CD31 in ischemic adductor muscles of both WT and 12/15-Lox$^{-/-}$ mice. It was observed that ischemia increased Hu177 cryptic collagen-positive staining in WT mice as compared with 12/15-Lox$^{-/-}$ mice (Fig. 8*E*).

DISCUSSION

Humans express 15-Lox1 and 15-Lox2, and both convert arachidonic acid to 15(*S*)-HETE as a predominant eicosanoid (50–53). Furthermore, the atherosclerotic arteries upon incubation with arachidonic acid produced 15(*S*)-HETE as a major eicosanoid (33, 34). Despite these observations, many studies have focused on the role of 12/15-Lox, a murine ortholog of 15-Lox1, in the pathogenesis of atherosclerosis and restenosis (24–26, 54), thus underscoring the importance of 15-Lox/15-HETE in these diseases. To understand the role of 15-Lox/15-HETE in vascular diseases, we have previously shown that it stimulates angiogenesis as well as the migration of smooth muscle cells (35–39, 52, 53). A role for angiogenesis in the progression of both atherosclerosis and restenosis has also been reported (55, 56). We have shown that 15(*S*)-HETE-induced angiogenesis requires induction of expression of angiogenic factors such as fibroblast growth factor, vascular endothelial growth factor, and interleukin-8 (35–37). MMPs have been reported to be involved in the progression of atherosclerosis and restenosis (13, 19, 57). Similarly, MMPs, particularly MMP-2, have been shown to be critical in the onset of tumor angiogenesis (58). The findings that atherosclerotic arteries produce 15-HETE as a major eicosanoid and it possesses the capacity to induce angiogenesis suggest that one of the mechanisms by which 15(*S*)-HETE could promote vascular diseases is via its involvement in the regulation of angiogenesis. Similarly, 15(*S*)-HETE via its capacity to induce MMP-2 expression and angiogenesis may be involved in tumor growth and metastasis as well.

FIGURE 4. **AP-1 (Fra-1/c-Jun) mediates 15(*S*)-HETE-induced MMP-2 expression and activity.** *A*, quiescent HDMVECs were treated with and without 15(*S*)-HETE (0.1 μM) for the indicated time periods, and cell extracts were prepared and analyzed by Western blotting for c-Fos, Fra-1, c-Jun, Jun-B, and β-tubulin levels using their respective antibodies. *B*, HDMVECs were transduced with Ad-GFP, Ad-dnRac1, Ad-dnMEK1, or Ad-dnJNK1 at 40 m.o.i., quiesced, treated with and without 15(*S*)-HETE (0.1 μM) for 1 h, and cell extracts were prepared and analyzed for either c-Fos, Fra-1, c-Jun, Jun-B, and β-tubulin levels or Fra-1 and c-Jun levels as described in *A*. The c-Jun blot was reprobed sequentially with anti-Rac1, anti-MEK1, or anti-JNK1 antibodies to show the overexpression of dnRac1, dnMEK1, and dnJNK1, respectively. *C*, HDMVECs were transfected with scrambled, Fra-1, or c-Jun siRNA, and 48 h later cell extracts were prepared and analyzed by Western blotting for Fra-1 and c-Jun levels using their specific antibodies. *D* and *E*, HDMVECs were transfected with scrambled, Fra-1, or c-Jun siRNA, quiesced, treated with and without 15(*S*)-HETE (0.1 μM) for 8 h, and either total cellular RNA was isolated and analyzed for MMP-2 and β-actin mRNA levels by QRT-PCR (*D*) or medium was collected and analyzed for MMP-2 activity by gelatin zymography (*E*). The *bar graphs* in *A–E* represent mean ± S.D. values of three independent experiments. *, $p < 0.01$ *versus* control or Ad-GFP or scrambled siRNA; †, $p < 0.01$ *versus* 15(*S*)-HETE or Ad-GFP plus 15(*S*)-HETE or scrambled siRNA plus 15(*S*)-HETE.

A

```
                                    AP-1                                                                    AP-1
-1704 ccctcccaag agggtccttt aaaacTGACT CTggaaagtc agagcacaca cccaccagac aagcctgaac ttgtctgaag cccACTGAGA cccaagccgc

-1604 agagactttt ctagctgtga tgatcaagac ataatcgtga cctccaatgc cccccacaag tatattgctc ctgattcttt cagcccctga ccttacttct

-1504 caaactgttc cctgctgacc cccagtccta tctgcccccc tcctaggctg gtccttactg acccctccag ctccatcccc tcaccctgtg ccccacctttt

-1404 ttcagataga aaaaactttc ttctccagtg cctcttgctg tttttcatct ctgggccatt gtcaatgttc cctaaaacat tccccatatt ccccacccag

                                          AP-1          STAT                                                CREB
-1304 cactccacct ctttagctct tcaggtctca gctcAGAAGT CActtcttcc aggaagcctt ccttgattgt ctttactagt ttaggggctg aagtcaggcg

-1204 ttcccaacag cctgctggag ttccccatca cagcttatct ctcaactgtc tttcctgaga gagggagaag acattcctca gagacggttg tcacagggag

-1104 aacttcaaaa ttgggattcg acctgagagg ccacatggat tcttggcttg gcgcaggaaa ggattcaaga gtgagtgggg aattcgtgga actgagggct

-1004 cctccccttt ttagaccata tagggtaaac ctccccacat tgccatggca tttatacact gccatggcac tggtgggtgc ttccctttaac atgctaatgc

 -904 attataatta gcgtaaaatg agcagtgagg atgaccagag gtcgctttct ttgccatctt ggttttggct ggcttcttca ctgcatactg ttttatcagt

 -804 ggggtctttg tgacctctat cttattaaac cagtcttgcc caatttctat ctcatcctgt gaccgagaat gcggaccctc ctgggagtgc agcccagcag

                    Sp-1
 -704 gtctcagcct cattttaccc agccccctgt tcaagatgga gtcgctctgg ttccaacgtc tctaacgcgg ggcccctgac tgctctattt cccaaggtgt

                                                                                    NFκB
 -604 atctagcatc tcgcactata cgaggccaag ttaaggctta cacatttgca gaaggaaaga ggtaaggaag caacctgggg ccttccactg tctctgtttc

 -504 catctctctc tttccatctc tgttcatccc agaatctctc tgtccctatc cctaaatatc gaaaatttct gtctctgacc atctatcatt gtggctgatc

 -404 atctgtttct gaccattcct tcccgttcct gaccccaggg agtgcagggt gtcctagcca agccggcgtc cctcctagta gtaccgctgc tctctaacct

      CREB
 -304 caggacgtca agggcctaga gcgacagatg tttcccagca gggggttctg aggctgtgcg cccagatcgc gagagaggca agtggggtga cgaggtcgtg

 -204 cactgagggt ggacgtagag gccaggagta gcaggcggcc ggggaaaaga ggtggagaaa ggaaaaaaga ggagaaaagt ggaggagggc gagtaggggg

                                          Sp-1
 -104 gtggggcaga gaggggcggg cccgagtgcg ccccccgccc ccagccccgc tctgccagct ccctcccagc ccagccggct acatctggcg gctgccctcc

   -4 cttgTTTCCG CTGCATCC
        └──►
         +1
```

B

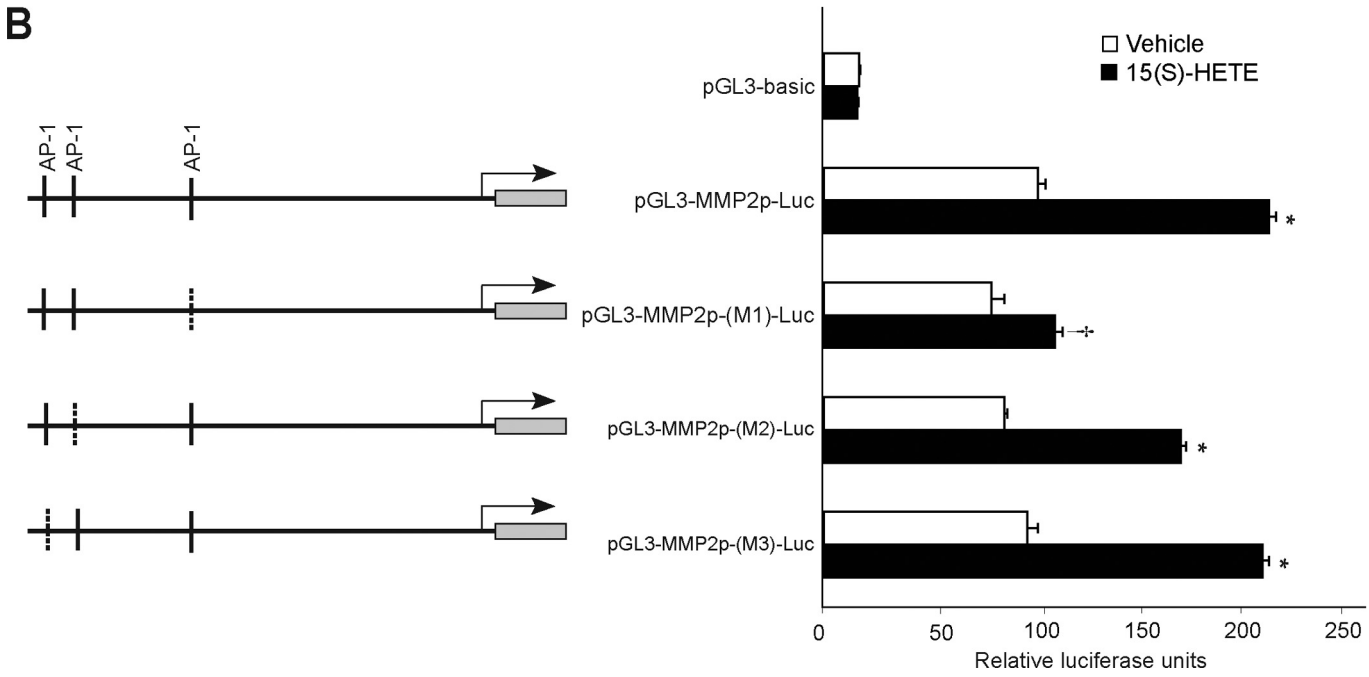

FIGURE 5. **15(*S*)-HETE-induced MMP-2 promoter-luciferase reporter gene activity requires −1263 AP-1-binding element.** *A*, sequence of the cloned 1.7-kb human MMP-2 promoter showing the −1263, −1615, and −1673 AP-1-binding sites. *B*, HDMVECs were transfected with empty vector (pGL3-basic) or MMP-2 promoter-luciferase constructs with and without site-directed mutagenesis of AP-1 sites, quiesced, and treated with and without 15(*S*)-HETE for 8 h, and cell extracts were prepared and analyzed for luciferase activity. *M1*, *M2*, and *M3* indicate mutations in AP-1 binding sites located at −1263, −1615, and −1673 nt, respectively. *, $p < 0.01$ *versus* vehicle control; †, $p < 0.01$ *versus* pGL3-MMP2p-Luc plus 15(*S*)-HETE. *Dotted vertical lines* indicate mutated AP-1 sites.

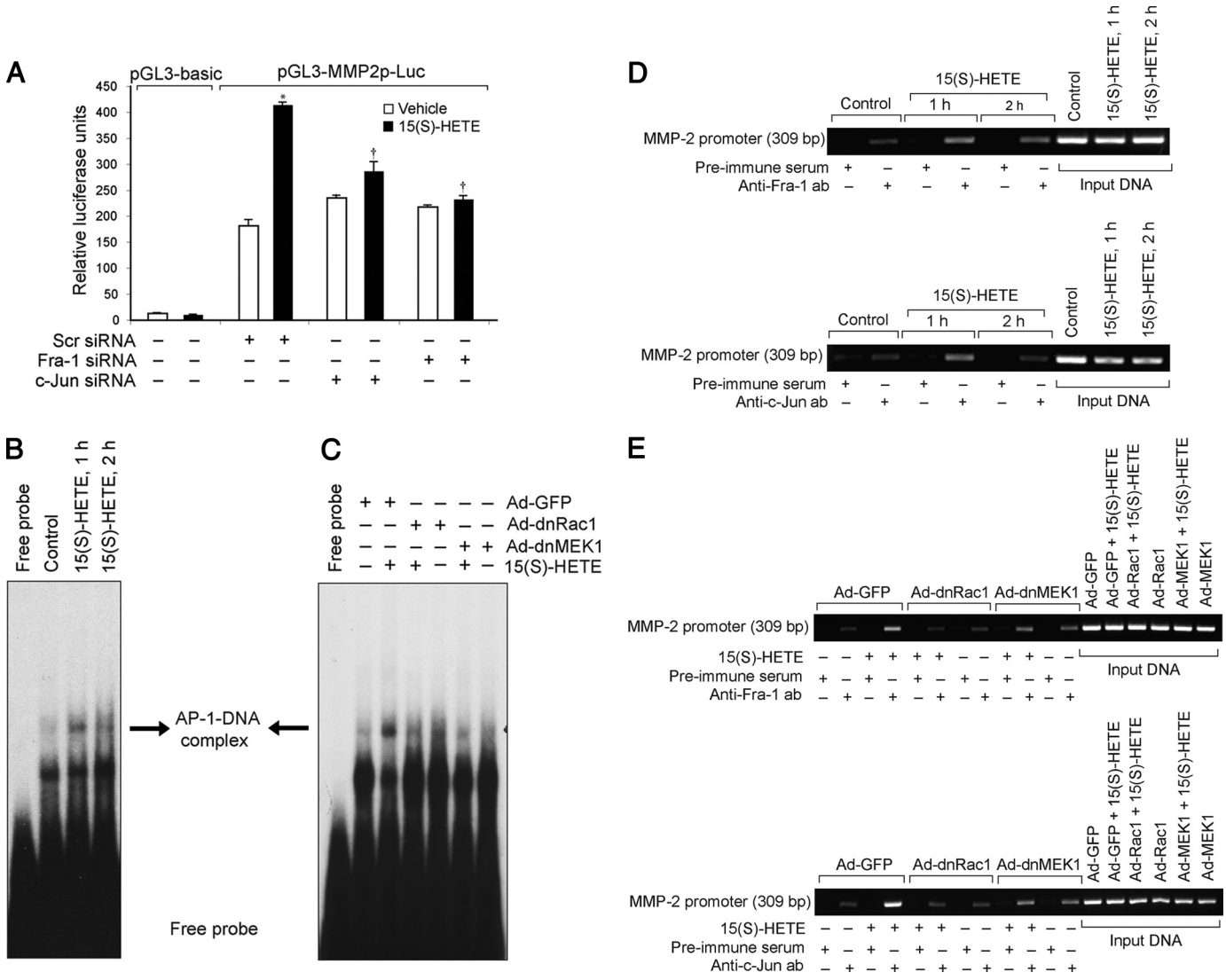

FIGURE 6. **Fra-1 and c-Jun bind to MMP-2 promoter in response to 15(*S*)-HETE in a Rac1- and MEK1-dependent manner.** *A*, HDMVECs were transfected with scrambled, Fra-1, or c-Jun siRNA in combination with empty vector or pGL3-MMP2p-Luc, quiesced, treated with and without 0.1 μM 15(*S*)-HETE for 8 h, and cell extracts were prepared and analyzed for luciferase activity. *B* and *D*, quiescent HDMVECs were treated with and without 15(*S*)-HETE (0.1 μM) for the indicated time periods, and either nuclear extracts were prepared and analyzed by EMSA for AP-1-binding activity using ^{32}P-labeled −1263 AP-1 binding sequence of MMP-2 promoter as a probe *in vitro* (*B*) or processed for ChIP analysis of Fra-1 and c-Jun binding to MMP-2 promoter *in vivo* using primers encompassing −1263 AP-1 site (*D*). *C* and *E*, HDMVECs were transduced with Ad-GFP, Ad-dnRac1, or Ad-dnMEK1 at 40 m.o.i., quiesced, and treated with and without 15(*S*)-HETE (0.1 μM) for 1 h, and either nuclear extracts were prepared and analyzed by EMSA for −1263 AP-1-binding activity as described in *B* (*C*) or processed for ChIP analysis of Fra-1 and c-Jun binding to MMP-2 promoter *in vivo* as described in *D* (*E*). *, $p < 0.01$ *versus* vehicle control; †, $p < 0.01$ *versus* pGL3-MMP2p-Luc plus 15(*S*)-HETE.

The Rho group of small GTPases plays a key role in cell motility (44, 45). In addition, Rac1 mediates MMP-2 activation by membrane type 1-MMP, and MMP-2 activity is required for Rac1-facilitated cell invasion across the type I collagen barrier (47). Because 15(*S*)-HETE stimulates Rac1 in the induction of expression of MMP-2, whose activation is needed for cell migration, it is logical to assume that the Rac-1-MMP-2 axis constitutes a motile signaling for endothelial cell invasion and migration in 15(*S*)-HETE-induced angiogenesis. Rac1 plays a role in mediating receptor tyrosine kinase and cytokine receptor signaling to activate JNK1 via recruiting MAPK kinase kinases, MEKK1–4, and MAPK kinases, MKK4/7 (59–61). Furthermore, activation of JNK1 is required for stimulus-induced expression of the Fos and Jun family of AP-1 transcriptional factors (62). Previously, we have shown that 15(*S*)-HETE activates JNK1 via Rac1-dependent stimulation of MEK1 (38). In the present study, we observed that activation of Rac1, MEK1, and JNK1 is required for 15(*S*)-HETE-induced Fra-1 and c-Jun expression in HDMVECs. Thus, these findings infer that, in addition to its role in F-actin stress fiber formation, Rac1 mediates signaling events leading to induction of expression of transcriptional factors such as Fra-1 and c-Jun in the stimulation of angiogenesis. In view of these observations, one can predict a crucial role for Rac1 in 15(*S*)-HETE-induced angiogenic responses of HDMVECs. Indeed, 15(*S*)-HETE-induced expression of MMP-2 requires Rac1-, MEK1-, and JNK1-mediated Fra-1-c-Jun/AP-1 activation. Thus, these findings clearly support a role for Rac1 in the mediation of 15(*S*)-HETE-induced angiogenesis.

The promoter regions of many MMPs, including MMP-1, -3, -7, -9, -10, -12, and -13, are highly conserved with respect to the ~7-bp AP-1 binding site (63). The functional significance of the AP-1 site in the mediation of MMP-2 promoter activity in response to hormones and cytokines such as angiotensin II,

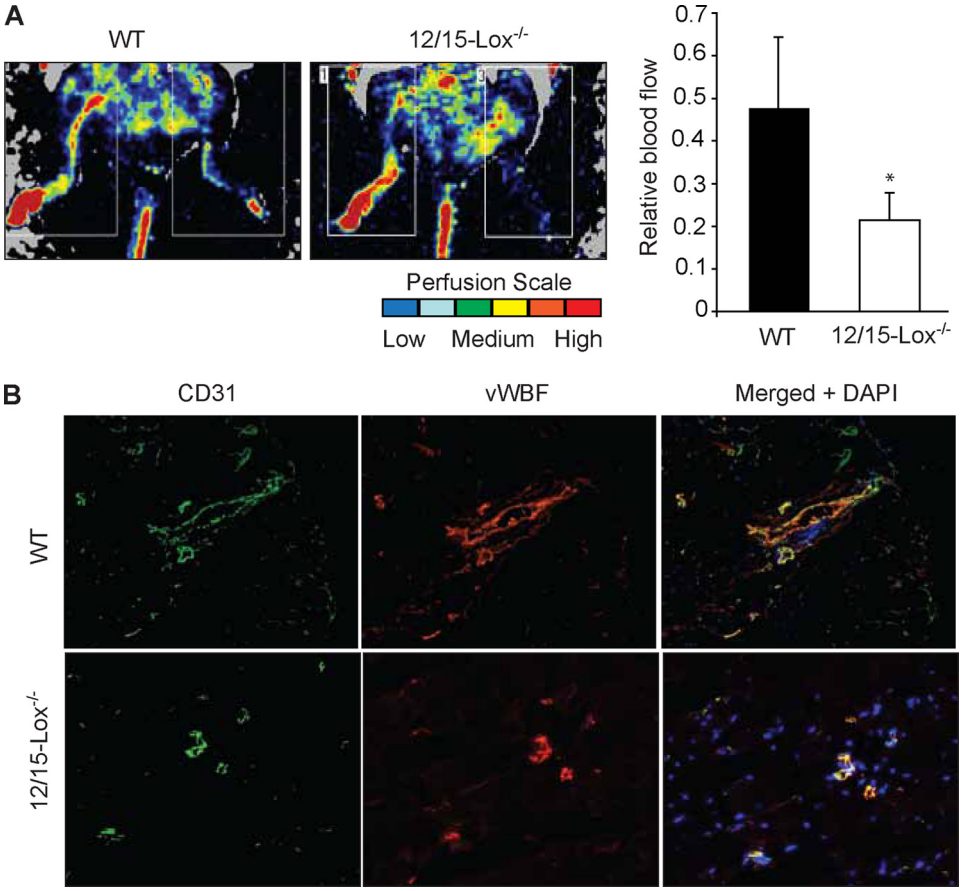

FIGURE 7. **Lack of 12/15-Lox gene impairs blood flow recovery after ischemia.** WT and 12/15-Lox$^{-/-}$ mice were subjected to hind limb ischemia by left femoral artery excision. *A*, on day 7 after hind limb ischemia, blood flow was measured by using laser Doppler perfusion imaging. Perfusion is expressed as the ratio of the ischemic to the non-ischemic hind limb. *B*, blood vessels in the ischemic adductor muscles of WT and 12/15-Lox$^{-/-}$ mice were analyzed by double immunofluorescence staining for CD31 (*green*) and vWF (*red*). *, $p < 0.01$ *versus* WT mice.

endothelin 1, and interleukin 1β was confirmed by EMSA studies and site-directed mutagenesis in cardiac cells (49). In addition, it was found that both Fra-1/Jun-B and Fos-B/Jun-B occupy the AP-1 site in the MMP-2 promoter in response to these stimulants. Although 15(*S*)-HETE induced c-Fos, Fra-1, Jun-B, and c-Jun levels very robustly, blockade of Rac1-MEK1 signaling suppressed predominantly Fra-1 and c-Jun levels indicating a possible role for these AP-1 components in the induction of MMP-2 expression. This assumption can be further corroborated by the findings that interference with JNK1 activation blocks 15(*S*)-HETE-induced Fra-1 and c-Jun levels. In addition, siRNA-mediated inhibition of Fra-1 or c-Jun levels led to a lack of effect of 15(*S*)-HETE on MMP-2 expression and its promoter activity. Interference with Rac1-MEK1 signaling negated the binding of these AP-1 transcriptional factors to MMP-2 promoter in response to 15(*S*)-HETE. Furthermore, data obtained by site-directed mutagenesis, EMSA, and ChIP assay suggest that, among the three AP-1 sites present in the 1.7-kb promoter, the AP-1 site proximal to the transcriptional start site is essential for 15(*S*)-HETE-induced MMP-2 promoter activity. Previous studies have demonstrated that MMPs by proteolytic degradation releases soluble ectodomain of fibroblast growth factor receptor-1 that possesses the capacity to bind to FGF (64). We observed that 15(*S*)-HETE induces the expression of FGF-2 (37, 38). These findings appear to be very intriguing and lead to the speculation that 15(*S*)-HETE while inducing the expression of FGF-2 may also via activation of MMPs release the soluble active ectodomain of its receptor so that the growth factor can bind and activate its receptor leading to angiogenesis. In this context, it is also noteworthy that MMPs and ADAMs (a disintegrin and metalloprotease) via releasing growth factors such as heparin-bound-EGF and heparin-bound-FGF from degradation of proteoglycans facilitates the activation of receptor tyrosine kinases by G-protein-coupled receptor agonists (65).

Neovascularization is an adaptive biological response of ischemia. Therefore, we have used a murine hind limb ischemia model to understand the physiological relevance of our *in vitro* findings on the role of 15(*S*)-HETE in the regulation of angiogenesis *in vivo* (41). It is interesting to note that in 12/15-Lox$^{-/-}$ mice the blood flow recovery is significantly lower than that in WT mice after hind limb ischemia suggesting a crucial role for 12(*S*)-HETE/15(*S*)-HETE in the stimulation of angiogenesis. MMP-mediated remodeling of extracellular matrix creates a permissive microenvironment for endothelial cell invasion and migration and thereby new blood vessel formation. Recently, it was shown that cryptic collagen epitope (Hu177) is present in both interstitial collagen type 1 and basement membrane collagen type IV and that selective exposure of these epitopes within ischemic muscle correlates with the enhanced MMP activity (42). Our findings reveal that 7 days after the initiation of ischemia, increased exposure of Hu177-positive staining was observed in the adductor muscles of WT mice suggesting increased MMP activity. In contrast, the adductor muscles of 12/15-Lox$^{-/-}$ mice showed decreased Hu177-positive staining as compared with WT mice, and this correlates with a lack of angiogenic response. These findings infer that 12/15-Lox and its metabolites of arachidonic acid, 12(*S*)-HETE/15(*S*)-HETE, are crucial in the induction of expression and activation of MMPs, most likely MMP-2, which is important for initiation of angiogenesis. Because exposure of Hu177-positive epitopes is a marker for increased MMP activities, including MMP-2 and MMP-9, our results may not exclude a possible role for other MMPs besides MMP-2 in 12(*S*)-HETE/15(*S*)-HETE-induced angiogenesis following ischemia. However, because ischemia mimicked 15(*S*)-HETE in the stimulation of MEK1 and JNK1 phosphorylation and induction of Fra-1, c-Jun, and MMP-2 expression, it is most likely that MMP-2 does play a role in ischemia-induced angiogene-

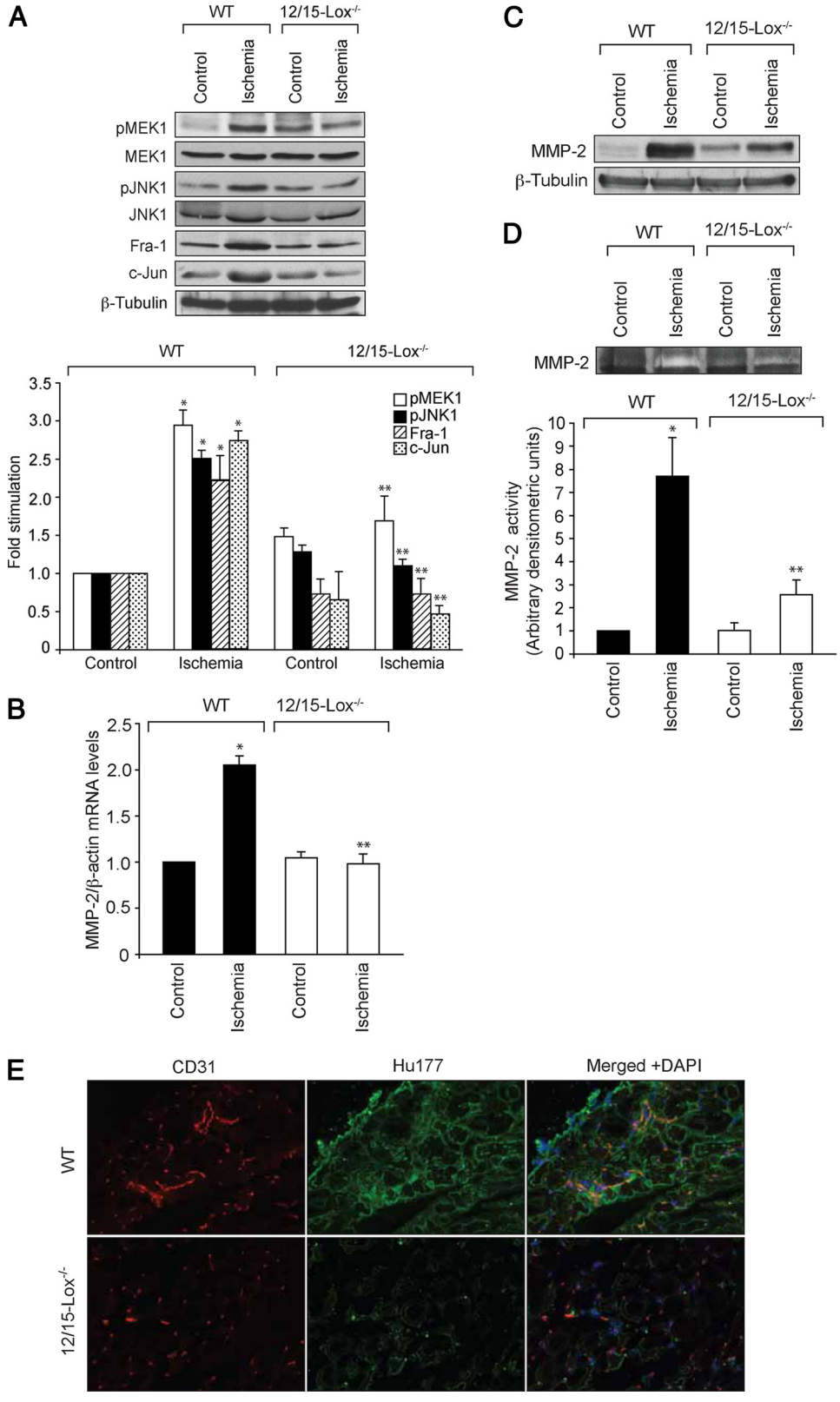

FIGURE 8. **Lack of 12/15-Lox gene impairs ischemia-induced MMP-2 expression and activity.** *A–D*, adductor muscles were isolated from ischemic and non-ischemic WT and 12/15-Lox$^{-/-}$ mice 7 days post-operation, and either tissue extracts were prepared or RNA was isolated. Tissue extracts were analyzed by Western blotting for MEK1 and JNK1 phosphorylation and Fra-1 and c-Jun levels using the respective antibodies (*A*). MMP-2 mRNA levels were measured by QRT-PCR (*B*), and its protein levels and activity were measured by Western blotting and gelatin zymography, respectively (*C* and *D*). *E*, cryptic collagen epitopes were evaluated in the ischemic adductor muscles of WT and 12/15-Lox$^{-/-}$ mice by immunofluorescence staining with anti-Hu177 antibodies (*green*) and anti-CD31 antibodies (*red*). The *bar graphs* in *A*, *B*, and *D* represent the mean ± S.D. values for six animals. *, $p < 0.01$ *versus* WT mice.

sis. Previous studies have reported that chronic hypoxia induces the expression of 15-Lox1 in aortic endothelial cells (66). We have shown that hypoxia induces the expression of 15-Lox1 in human microvascular endothelial cells and thereby increases the production of 15(*S*)-HETE (37). The hypoxia-induced expression of 15-Lox1 and the production of its arachidonic acid metabolite, 15(*S*)-HETE, may be attributed to its adaptive role in restoring the blood flow to ischemic tissues as observed in the present study. The lack of angiogenic response following mild ischemia in 12/15-Lox$^{-/-}$ mice is consistent with this assumption. In contrast to these observations, some recent reports have shown that 15-Lox1 inhibits vascular endothelial growth factor-A and placental growth factor-induced angiogenesis in rabbit skeletal muscle (67). These differential effects of 15-Lox1–15-HETE axis in the modulation of angiogenesis may be attributed to species variations.

Taken together, our studies provide a mechanistic evidence for the role of 12/15(*S*)-HETE in the regulation of angiogenesis through Rac1, MEK1, JNK1, and AP-1 (Fra-1/c-Jun)-dependent expression and secretion of MMP-2. We have previously reported that 15(*S*)-HETE-induced angiogenesis requires the production of FGF-2, vascular endothelial growth factor, and interleukin-8 (35, 36, 68). Because angiogenesis is an orchestrated cellular process involving the actions of many molecules, it is quite expected that 15(*S*)-HETE-induced angiogenesis may also need the requirement of several molecules, including cytokines and MMPs. Based on the capacity of 15(*S*)-HETE to stimulate angiogenesis and its production in atherosclerotic arteries as a major eicosanoid, it is likely that this oxidized lipid molecule contributes to the pathological angiogenesis that occurs in atherosclerotic plaques and restenotic lesions.

REFERENCES

1. Folkman, J. (1995) *Nat. Med.* **1,** 27–31
2. Freedman, S. B., and Isner, J. M. (2001) *J. Mol. Cell Cardiol.* **33,** 379–393
3. Mignatti, P., and Rifkin, D. B. (1996) *Enzyme Protein* **49,** 117–137
4. Lauer-Fields, J. L., Sritharan, T., Stack, M. S., Nagase, H., and Fields, G. B. (2003) *J. Biol. Chem.* **278,** 18140–18145
5. Gross, J., and Lapiere, C. M. (1962) *Proc. Natl. Acad. Sci. U.S.A.* **48,** 1014–1022
6. Vu, T. H., and Werb, Z. (2000) *Genes Dev.* **14,** 2123–2133
7. Stefanidakis, M., and Koivunen, E. (2006) *Blood* **108,** 1441–1450
8. Shi, J., Son, M. Y., Yamada, S., Szabova, L., Kahan, S., Chrysovergis, K., Wolf, L., Surmak, A., and Holmbeck, K. (2008) *Dev. Biol.* **313,** 196–209
9. Roy, R., Zhang, B., and Moses, M. A. (2006) *Exp. Cell Res.* **312,** 608–622
10. Visse, R., and Nagase, H. (2003) *Circ. Res.* **92,** 827–839
11. Deryugina, E. I., and Quigley, J. P. (2006) *Cancer Metastasis Rev.* **25,** 9–34
12. Mohammed, F. F., Smookler, D. S., and Khokha, R. (2003) *Ann Rheum. Dis.* **62,** Suppl. 2, ii43–47
13. Dollery, C. M., McEwan, J. R., and Henney, A. M. (1995) *Circ. Res.* **77,** 863–868
14. Galis, Z. S., and Khatri, J. J. (2002) *Circ. Res.* **90,** 251–262
15. Creemers, E. E., Cleutjens, J. P., Smits, J. F., and Daemen, M. J. (2001) *Circ. Res.* **89,** 201–210
16. Spinale, F. G. (2002) *Circ. Res.* **90,** 520–530
17. Fatar, M., Stroick, M., Griebe, M., and Hennerici, M. (2005) *Cerebrovasc. Dis.* **20,** 141–151
18. Coker, M. L., Doscher, M. A., Thomas, C. V., Galis, Z. S., and Spinale, F. G. (1999) *Am. J. Physiol.* **277,** H777–H787
19. Galis, Z. S., Muszynski, M., Sukhova, G. K., Simon-Morrissey, E., Unemori, E. N., Lark, M. W., Amento, E., and Libby, P. (1994) *Circ. Res.* **75,** 181–189
20. Hanemaaijer, R., Koolwijk, P., le Clercq, L., de Vree, W. J., and van Hinsbergh, V. W. (1993) *Biochem. J.* **296,** 803–809
21. Alexander, S. M., Jackson, K. J., Bushnell, K. M., and McGuire, P. G. (1997) *Dev. Dyn.* **209,** 261–268
22. Linask, K. K., Han, M., Cai, D. H., Brauer, P. R., and Maisastry, S. M. (2005) *Dev. Dyn.* **233,** 739–753
23. Linask, K. K., Manisastry, S., and Han, M. (2005) *Microsc. Microanal.* **11,** 200–208
24. Cyrus, T., Witztum, J. L., Rader, D. J., Tangirala, R., Fazio, S., Linton, M. F., and Funk, C. D. (1999) *J. Clin. Invest.* **103,** 1597–1604
25. Zhao, L., and Funk, C. D. (2004) *Trends Cardiovasc. Med.* **14,** 191–195
26. Poeckel, D., Zemski Berry, K. A., Murphy, R. C., and Funk, C. D. (2009) *J. Biol. Chem.* **284,** 21077–21089
27. Kelavkar, U. P., Glasgow, W., Olson, S. J., Foster, B. A., and Shappell, S. B. (2004) *Neoplasia.* **6,** 821–830
28. Gonzalez, A. L., Roberts, R. L., Massion, P. P., Olson, S. J., Shyr, Y., and Shappell, S. B. (2004) *Hum. Pathol.* **35,** 840–849
29. Preston, I. R., Hill, N. S., Warburton, R. R., and Fanburg, B. L. (2006) *Am. J. Physiol. Lung Cell Mol. Physiol.* **290,** L367–374
30. Dronadula, N., Rizvi, F., Blaskova, E., Li, Q., and Rao, G. N. (2006) *J. Lipid Res.* **47,** 767–777
31. Li, Y., Li, Q., Wang, Z., Liang, D., Liang, S., Tang, X., Guo, L., Zhang, R., and Zhu, D. (2009) *Apoptosis* **14,** 42–51
32. Calandria, J. M., Marcheselli, V. L., Mukherjee, P. K., Uddin, J., Winkler, J. W., Petasis, N. A., and Bazan, N. G. (2009) *J. Biol. Chem.* **284,** 17877–17882
33. Henriksson, P., Hamberg, M., and Diczfalusy, U. (1985) *Biochim. Biophys. Acta* **834,** 272–274
34. Simon, T. C., Makheja, A. N., and Bailey, J. M. (1989) *Atherosclerosis* **75,** 31–38
35. Srivastava, K., Kundumani-Sridharan, V., Zhang, B., Bajpai, A. K., and Rao, G. N. (2007) *Cancer Res.* **67,** 4328–4336
36. Cheranov, S. Y., Wang, D., Kundumani-Sridharan, V., Karpurapu, M., Zhang, Q., Chava, K. R., and Rao, G. N. (2009) *Blood* **113,** 6023–6033
37. Zhang, B., Cao, H., and Rao, G. N. (2005) *Cancer Res.* **65,** 7283–7291
38. Zhao, T., Wang, D., Cheranov, S. Y., Karpurapu, M., Chava, K. R., Kundumani-Sridharan, V., Johnson, D. A., Penn, J. S., and Rao, G. N. (2009) *J. Lipid Res.* **50,** 521–533
39. Bajpai, A. K., Blaskova, E., Pakala, S. B., Zhao, T., Glasgow, W. C., Penn, J. S., Johnson, D. A., and Rao, G. N. (2007) *Invest. Ophthalmol. Vis. Sci.* **48,** 4930–4938
40. Bian, J., and Sun, Y. (1997) *Mol. Cell. Biol.* **17,** 6330–6338
41. Yu, J., deMuinck, E. D., Zhuang, Z., Drinane, M., Kauser, K., Rubanyi, G. M., Qian, H. S., Murata, T., Escalante, B., and Sessa, W. C. (2005) *Proc. Natl. Acad. Sci. U.S.A.* **102,** 10999–11004
42. Gagne, P. J., Tihonov, N., Li, X., Glaser, J., Qiao, J., Silberstein, M., Yee, H., Gagne, E., and Brooks, P. (2005) *Am J. Pathol.* **167,** 1349–1359
43. Droppelmann, C. A., Gutiérrez, J., Vial, C., and Brandan, E. (2009) *J. Biol. Chem.* **284,** 13551–13561
44. Etienne-Manneville, S., and Hall, A. (2002) *Nature* **420,** 629–635
45. Raftopoulou, M., and Hall, A. (2004) *Dev. Biol.* **265,** 23–32
46. Liu, W. F., Nelson, C. M., Pirone, D. M., and Chen, C. S. (2006) *J. Cell Biol.* **173,** 431–441
47. Zhuge, Y., and Xu, J. (2001) *J. Biol. Chem.* **276,** 16248–16256
48. Benbow, U., and Brinckerhoff, C. E. (1997) *Matrix Biol.* **15,** 519–526
49. Bergman, M. R., Cheng, S., Honbo, N., Piacentini, L., Karliner, J. S., and Lovett, D. H. (2003) *Biochem. J.* **369,** 485–496
50. Sigal, E., Craik, C. S., Highland, E., Grunberger, D., Costello, L. L., Dixon, R. A., and Nadel, J. A. (1988) *Biochem. Biophys. Res. Commun.* **157,** 457–464
51. Brash, A. R., Boeglin, W. E., and Chang, M. S. (1997) *Proc. Natl. Acad. Sci. U.S.A.* **94,** 6148–6152
52. Potula, H. S., Wang, D., Quyen, D. V., Singh, N. K., Kundumani-Sridharan, V., Karpurapu, M., Park, E. A., Glasgow, W. C., and Rao, G. N. (2009) *J. Biol. Chem.* **284,** 31142–31155
53. Chava, K. R., Karpurapu, M., Wang, D., Bhanoori, M., Kundumani-Sridharan, V., Zhang, Q., Ichiki, T., Glasgow, W. C., and Rao, G. N. (2009) *Arterioscler. Thromb. Vasc. Biol.* **29,** 809–815
54. Gu, J. L., Pei, H., Thomas, L., Nadler, J. L., Rossi, J. J., Lanting, L., and Natarajan, R. (2001) *Circulation* **103,** 1446–1452
55. Koutouzis, M., Nomikos, A., Nikolidakis, S., Tzavara, V., Andrikopoulos, V., Nikolaou, N., Barbatis, C., and Kyriakides, Z. S. (2007) *Atherosclerosis* **192,** 457–463
56. Khurana, R., Zhuang, Z., Bhardwaj, S., Murakami, M., De Muinck, E., Yla-Herttuala, S., Ferrara, N., Martin, J. F., Zachary, I., and Simons, M. (2004) *Circulation* **110,** 2436–2443
57. Zahradka, P., Harding, G., Litchie, B., Thomas, S., Werner, J. P., Wilson, D. P., and Yurkova, N. (2004) *Am. J. Physiol. Heart Circ. Physiol.* **287,** H2861–H2870
58. Thaker, P. H., Han, L. Y., Kamat, A. A., Arevalo, J. M., Takahashi, R., Lu, C., Jennings, N. B., Armaiz-Pena, G., Bankson, J. A., Ravoori, M., Merritt, W. M., Lin, Y. G., Mangala, L. S., Kim, T. J., Coleman, R. L., Landen, C. N., Li, Y., Felix, E., Sanguino, A. M., Newman, R. A., Lloyd, M., Gershenson, D. M., Kundra, V., Lopez-Berestein, G., Lutgendorf, S. K., Cole, S. W., and Sood, A. K. (2006) *Nat. Med.* **12,** 939–944
59. Davis, R. J. (2000) *Cell* **103,** 239–252
60. Minden, A., Lin, A., Claret, F. X., Abo, A., and Karin, M. (1995) *Cell* **81,** 1147–1157
61. Teramoto, H., Coso, O. A., Miyata, H., Igishi, T., Miki, T., and Gutkind, J. S. (1996) *J. Biol. Chem.* **271,** 27225–27228
62. Ventura, J. J., Kennedy, N. J., Lamb, J. A., Flavell, R. A., and Davis, R. J. (2003) *Mol. Cell. Biol.* **23,** 2871–2882
63. Vincenti, M. P. (2001) *Methods Mol. Biol.* **151,** 121–148
64. Levi, E., Fridman, R., Miao, H. Q., Ma, Y. S., Yayon, A., and Vlodavsky, I. (1996) *Proc. Natl. Acad. Sci. U.S.A.* **93,** 7069–7074
65. Gschwind, A., Hart, S., Fischer, O. M., and Ullrich, A. (2003) *EMBO J.* **22,** 2411–2421
66. Zhu, D., Medhora, M., Campbell, W. B., Spitzbarth, N., Baker, J. E., and Jacobs, E. R. (2003) *Circ. Res.* **92,** 992–1000
67. Viita, H., Markkanen, J., Eriksson, E., Nurminen, M., Kinnunen, K., Babu, M., Heikura, T., Turpeinen, S., Laidinen, S., Takalo, T., and Ylä-Herttuala, S. (2008) *Circ. Res.* **102,** 177–184
68. Kundumani-Sridharan, V., Niu, J., Wang, D., Van Quyen, D., Zhang, Q., Singh, N. K., Subramani, J., Karri, S., and Rao, G. N. (2010) *Blood* **115,** 2105–2116